

Partial draining of a tethered polymer in flow

R. RZEHA¹, D. KIENLE¹, T. KAWAKATSU² and W. ZIMMERMANN^{1,3}

¹ *FORUM and IFF, Forschungszentrum Jülich - D-52425 Jülich, Germany*

² *Dept. Compt. Sci. Eng., Nagoya University - Nagoya 464-8603, Japan*

³ *Theoretische Physik, Universität des Saarlandes - D-66041 Saarbrücken, Germany*

(received 28 January 1999; accepted in final form 30 March 1999)

PACS. 83.10Nn – Polymer dynamics.

PACS. 83.20Di – Microscopic (molecular) theories.

PACS. 47.50+d – Non-Newtonian fluid flows.

Abstract. – Deformations of a polymer fixed at one end and subjected to a uniform flow are investigated with special emphasis on the hydrodynamic interaction (HI) between polymer segments. The so-called non-draining effect, which results from the collective hydrodynamic back-flow caused by all segments, is calculated for the first time with fluctuating hydrodynamic interactions. HI reduces the viscous drag and the flow partially penetrates the polymer coil. Therefore neither the free-draining nor the non-draining models discussed previously describe the polymer-flow interaction appropriately. Accordingly the *f*-shell blob model is introduced, describing the partial draining and the transition to a free-draining polymer with increasing flow velocity, similarly as in simulations.

Introduction. – Non-Newtonian fluids exhibit astonishing flow behavior such as turbulent drag reduction in dilute polymer solutions [1, 2] and their understanding is both theoretically challenging and of high technological importance. However, a generally accepted theoretical basis for the description of the large-scale motion of non-Newtonian fluids, similar to the Navier-Stokes equations for simple fluids, is not available yet. Only for small displacement gradients there is a broadly accepted “general linear viscoelastic model” for incompressible viscoelastic fluids [2, 3], where the parameters can be determined by standard rheological techniques. This approach is also sufficient to predict instabilities in hydrodynamic systems, such as the Faraday instability, when only small deformations of the fluid are involved [4]. But the understanding of the *non-linear* behavior of non-Newtonian fluids is much less advanced and it requires a thorough analysis of the interplay between flows and polymers. Accordingly two basic questions are addressed in this work: How does the flow field deform a tethered polymer and how is the flow field modified by the presence of the polymer?

In classical experiments on the dynamics of polymers in solution such as light scattering, birefringence, rheometry and small-angle neutron scattering one measures only volume-averaged quantities. A huge step forward in the analysis of the crucial interplay between the flow field and the deformations of the polymers has been achieved by studying single DNA molecules. DNA is much larger than synthetic polymers like polyethylene(-oxide) and can be manipulated with optical tweezers. When decorated by fluorescent dyes, the action of flows on the polymer can be followed under an optical microscope [5].

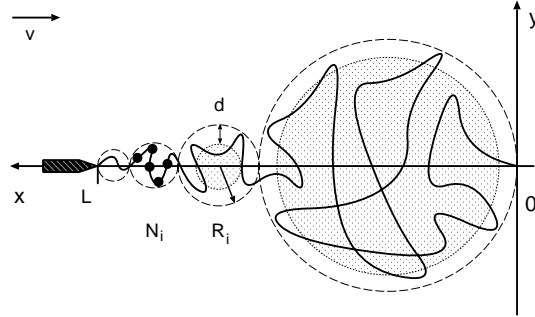


Fig. 1. – Sketch of a polymer tethered at one end and exposed to a uniform flow field with velocity \mathbf{v} . In the blob picture the deformed polymer with N segments (beads) is approximated by a sequence of spheres (blobs) with radius R_i and containing N_i segments. In the f -shell blob model each blob consists of a free-draining outer shell of thickness d and an impenetrable inner sphere (shaded).

Here we report on 3-dimensional computer simulations of bead-spring models for a tethered polymer as sketched in fig. 1. The models include the hydrodynamic interaction (HI) between the polymer segments as well as the excluded-volume interaction (EVI) [2,3], but unlike other work [6] we avoid averaging approximations in the treatment of the HI. For the first time the polymer-induced perturbation of the flow is determined, which is no less important for the behavior of non-Newtonian fluids than the flow-induced deformation of the polymer. We found in simulations that HI reduces the flow-induced drag force on the polymer and that the flow partially penetrates the polymer coil. In contrast former models assume non-draining polymers [7]. In order to cover the partial draining, we introduce a generalized blob model with blobs having a free-draining outer shell and a non-draining inner sphere. Consequently this model is able to describe a transition between a coiled, nearly impenetrable polymer and a nearly stretched free-draining polymer. In addition the dependence of the polymer elongation on the flow velocity is changed compared to previous models, and it is closer to results from our simulations.

Bead-spring model. – In our simulations we follow the Brownian dynamics of a bead-spring model as described in more detail in refs. [8,9], where the equation of motion for the vector $\mathbf{R} = (\mathbf{R}_1, \dots, \mathbf{R}_N)$ of all bead positions may be written in the form

$$\dot{\mathbf{R}} = \mathbf{v} + \mathbf{H} \mathbf{F} + \sqrt{2k_B T} \mathbf{H} \xi. \quad (1)$$

Here k_B is the Boltzmann constant, T the temperature and $\xi(\mathbf{R}, t)$ is uncorrelated Gaussian white noise with zero mean. The potential forces \mathbf{F} comprise a repulsive Lennard-Jones interaction [10] describing the EVI and the next-neighbor bond forces for which we use either a harmonic force law or the familiar FENE (Finite Extensible Nonlinear Elastic) force [11]. The latter provides a reasonable approximation of polymers with a fixed contour length unless the external flow velocity becomes very large. The parameters appearing in the potential forces \mathbf{F} have been chosen as in ref. [11] where this choice was shown to prohibit bond crossings. The hydrodynamic interactions are incorporated in the Oseen tensor approximation [2,3]. In this case the flow perturbations due to all beads simply superimpose and the additional drag forces can be expressed by the non-diagonal part of the mobility tensor \mathbf{H} . We have $H_{ij} = \Omega(\mathbf{R}_i - \mathbf{R}_j)$ for $i \neq j$, with $\Omega(\mathbf{r}) = (\mathbf{1} + \hat{\mathbf{r}}\hat{\mathbf{r}}^T)/(8\pi\eta|\mathbf{r}|)$ and $H_{ii} = \mathbf{1}/\zeta$, with $\zeta = 6\pi\eta a$ being the friction coefficient of a bead with radius a in a solvent with viscosity η . In contrast to previous works [6] we do not average \mathbf{H} . For instance, the preaveraged mobility tensor \mathbf{H}

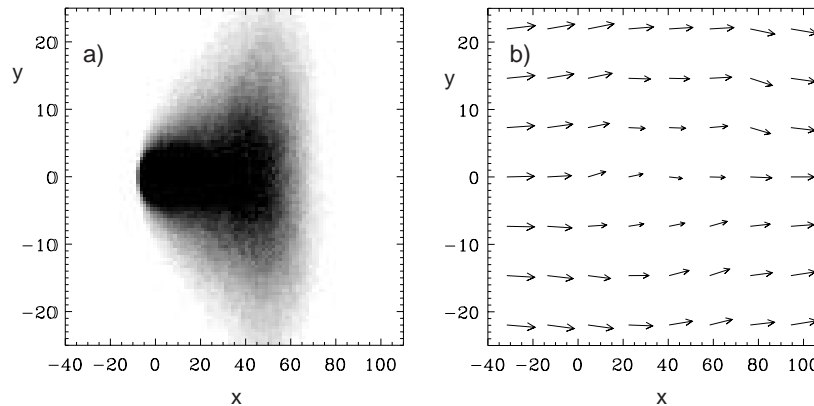


Fig. 2. – Segment density $\rho(x, y, z = 0)$ (a) and time-averaged perturbed flow field $\mathbf{u}(x, y, z = 0)$ (b) for a chain with $N = 200$ segments which is fixed at the origin with one end and subjected to a uniform flow in the x -direction with $v = 0.02$. Both EVI and HI are included and harmonic springs are used. The streamlines go around the region where the density of polymer segments is high.

in the Zimm model [12] becomes independent of \mathbf{R} so that eq. (1) becomes a linear equation, if in addition linear springs are assumed and EVI is neglected. The values $\eta = 0.2$, $\zeta = 1.0$, $k_B T = 1.0$ and $b = 1.0$ (harmonic springs) or $b = 0.961$ (FENE springs) for the bondlength b fix the strength of the HI and the units of force, energy, length etc.

Results. – The temporally averaged segment density of a tethered bead-spring chain with harmonic springs and $N = 200$ beads is shown in fig. 2 for a uniform imposed flow with velocity $v = 0.02$. The full flow field $\mathbf{u}(\mathbf{r})$ including the perturbation due to the HI between the beads is shown in fig. 2b). The y -dependence of $u_x(\mathbf{r})$, as shown in fig. 3a), indicates a non-vanishing flow at the average location of the polymer coil. This flow penetration is a superposition of two effects: The flow penetrates the polymer coil at any moment and due to thermal fluctuations the polymer does not stay at a fixed location. The root-mean-square end-to-end distance R_E as a measure for the polymer extension in flow direction is plotted in fig. 3b). Without HI (upper curve) we find in the velocity range $v = 0.001$ – 0.01 a power law $R_E \propto v^\mu$ with $\mu = 0.5$ and a transition to a linear dependence $R_E \propto v$ beyond $v > 0.1$. Beyond this crossover EVI becomes negligible because the polymer is uncoiled at large flow velocities. Including HI (lower curve) there is around $v = 0.5$ a maximal exponent of $\mu = 1.5$ which is larger than without HI. The extension of a FENE chain with and without HI is shown in fig. 4a). For both chains with harmonic or FENE springs, HI reduces the *drag force* exerted by the whole polymer on the tether point. This reduced *viscous drag* shifts the unwinding of the polymer with HI to larger values of the imposed flow velocity, as shown in fig. 3b) and fig. 4a). R_E for a FENE chain with and without HI is still different for large values of v , because the non-linear springs keep neighbouring beads close together so that the HI between next neighbours along the chain never becomes negligible. In contrast, harmonic springs become strongly stretched at large values of v and HI effects tend to zero, which is the reason for the convergence of the two curves in fig. 3b).

$R_E(v)$ may be compared with analytical scalings for blob models, where the chain is described by a sequence of impenetrable [7] or free-draining blobs [9]. For free-draining chains with harmonic springs there is reasonable agreement with results for a blob model [9]. However, for impenetrable blobs $R_E(v) \propto v^\mu$ with $\mu = 2$ is predicted [7], which is considerably larger

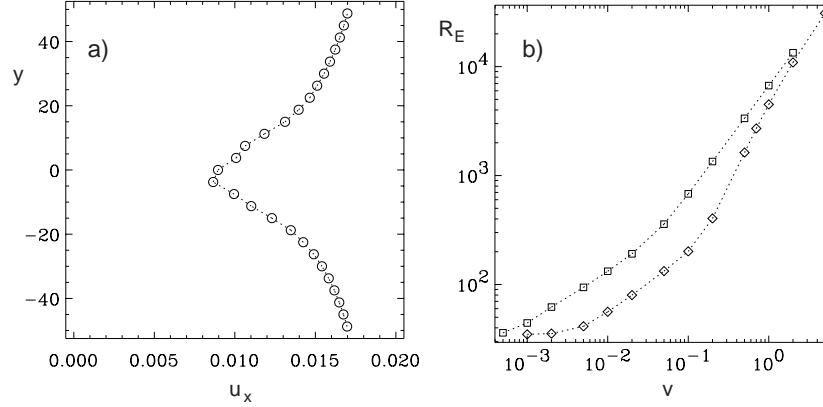


Fig. 3. – a) Spatially averaged x -component of the velocity field \mathbf{u} shown in fig. 2b) as a function of y . The average was taken over the range $0 \leq x \leq 40$ where the segment density is large. b) Root-mean-square end-to-end distance as a function of the imposed velocity v both with HI (lower curve) and without HI (upper curve). Otherwise the same model as in fig. 2 was used.

than the maximal exponent $\mu \sim 1.5$ of the lower curve in fig. 3b). There are several reasons for deviations between simulations and blob models. First of all a scaling regime as for the blob model is possible only for much longer chains than in present simulations with EVI or HI. Without EVI and HI, random flight and FENE chains can be analyzed semi-analytically [9]. This analysis shows that rather long chains with a number of more than $N \sim 2000$ beads are required to get a small velocity range where $R_E(v)$ shows a scaling behavior as predicted by the free-draining blob model [9]. Secondly, when the polymer uncoils with increasing flow velocity, EVI and HI effects are continuously “switched off”. This inhomogeneous process, starting at the tether point and extending to the free end with increasing flow velocity, is not described by the blob models considered so far.

f-shell blob model. – The partial penetration of flow into the polymer coil may be taken into account in blob models by assuming for each blob a free-draining outer shell of thickness d and an impenetrable inner sphere, cf. fig. 1. The previously discussed non-draining [7] and free-draining blob models [9] are limiting cases of this *f-shell* blob model. According to the Pincus rule [13], the radius R_k of a blob is determined by a balance between the total force F_k acting on it and the thermal agitation, $R_k = k_B T / F_k$. The radius of the non-draining inner sphere is $R_k^{\text{non}} = R_k - d$. Using the Flory scaling $R_k = b N_k^\nu$, the number of segments $N_k = (R_k/b)^{1/\nu}$ within the k -th blob may be calculated as well as the number of segments in the non-draining core and in the outer free-draining shell: $N_k^{\text{non}} = [(R_k - d)/b]^{1/\nu}$ and $N_k^{\text{free}} = N_k - N_k^{\text{non}}$. F_k is the sum of drag forces exerted by the $(k-1)$ blobs counted from the free end plus the Stokes friction acting on the k -th blob caused by both the non-draining inner sphere and by the free-draining shell, *i.e.* $F_k = F_{k-1} + 6\pi\eta v R_k^{\text{non}} + 6\pi\eta a v N_k^{\text{free}}$. Here a is the effective hydrodynamic bead radius. Together this provides the recursion relation for the force F_k

$$F_k = F_{k-1} + 6\pi\eta v \left(\frac{k_B T}{F_k} - d \right) + \frac{6\pi\eta v a}{b^{1/\nu}} \left(\left(\frac{k_B T}{F_k} \right)^{1/\nu} - \left(\frac{k_B T}{F_k} - d \right)^{1/\nu} \right), \quad (2)$$

with the boundary condition $F_0 = 0$. Via the Pincus rule the radii $R_k = k_B T / F_k$ are given and their sum $\sum_k R_k$ is the overall extension $L(v)$ of a polymer as a function of the velocity,

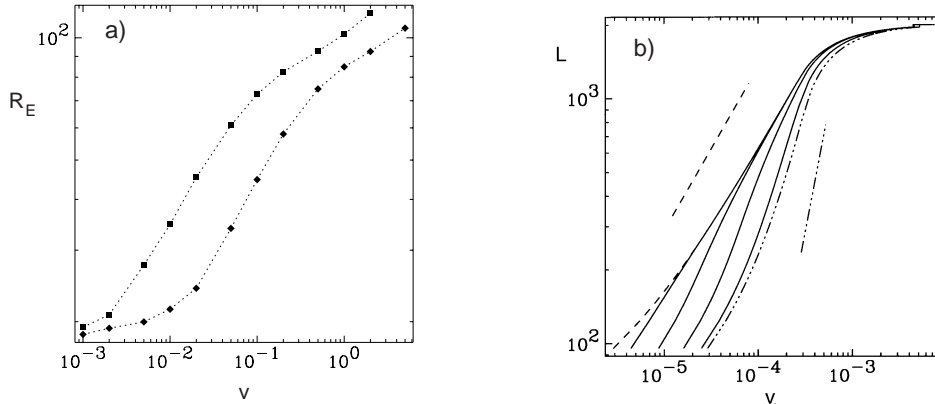


Fig. 4. – a) Root-mean-square end-to-end distance $R_E(v)$ from simulations of a FENE chain with $N = 100$ segments with (lower curve) and without HI (upper curve). b) Elongation $L(v)$ for the f -shell blob model with various values of the penetration depth $d = 1.0, 5.0, 15.0, 40.0$ from right to left. The straight lines are the power laws obtained for analytical approximations. The dash-dotted curve is for the non-draining limit $d = 0$ while the dashed line corresponds to the free-draining limit $d = R_F$. Parameters are $N = 2000$ and $b = 1.0$ corresponding to $R_F = bN^{3/5} = 95.6$ and $a = 0.48$ has been chosen such that for these parameters, the polymer elongation starts already at smaller velocities in the free-draining limit (dashed) than in the non-draining limit (dash-dotted), similarly as in our simulations.

cf. fig. 4. If $R_k < d$ the k -th blob is completely free-draining and the factor $\frac{k_B T}{F_k} - d$ in eq. (2) vanishes. For all blobs with $R_k \leq b$ we have $N_k = 1$ and R_k is replaced by b . This latter part of the chain forms the stem [7]. The intermediate curves in fig. 4 (solid lines) are for different values of the penetration depth d . In the non-draining and the free-draining limits eq. (2) may be solved analytically with some approximations [7, 9]. Then one obtains simple power laws for the polymer extension: $L(v) \sim v^2$ in the non-draining limit [7] and $L(v) \sim v^{2/3}$ in the free-draining limit [9], when $\nu = 3/5$ is chosen in the Flory relation. However, an exact numerical calculation of $L(v)$, as shown in fig. 4 by the dashed and the dash-dotted curves, has more structure than the simple power laws obtained by the approximate calculation, cf. straight lines in fig. 4. The analytical power laws may be considered as upper limits for the slope $L(v)$ for very long chains. A finite penetration depth d gives an even smaller slope $L(v)$ than for $d = 0$, as shown in fig. 4. According to both effects one cannot expect any scaling regime with simple power laws for $L(v)$ for molecules having less than $N \sim 1500$ – 2000 Kuhn segments which are used in experiments.

Discussion and conclusion. – The 3D simulation of a bead-spring model for a tethered polymer in uniform flow, as described in this letter, allows a detailed monitoring of various interactions between chain segments at different stages of the polymer deformation. For a polymer at thermal equilibrium it is well known that HI does not affect its shape and EVI leads to a swelling of the polymer (see *e.g.* [3]). At an intermediate flow velocity the HI leads to a reduction of the drag force exerted on the polymer compared to a chain without HI, cf. fig. 3b) and fig. 4a). Accordingly the elongation is smaller for a chain where HI is taken into account. The flow partially penetrates into a coiled polymer, cf. fig. 2b) and fig. 3a), in contrast to models assuming non-draining polymers. With increasing elongation the polymer becomes free-draining because HI and EVI are gradually “switched off” with the increasing distance between different parts of the polymer. However, due to the correlation caused by HI

the drag force on unstretchable polymers is smaller with HI than without, even at very high flow velocities.

In conclusion, the variation of HI and EVI along a flow-deformed polymer must be considered carefully in coarse-grained models of polymers, such as blob models or dumbbell models. The common dumbbell models do not describe spatially dependent interactions. Blob models [7] may be generalized appropriately to describe the variation of HI along the chain and the transition to a free-draining polymer taking place with increasing deformation. In order to do so, we have chosen the simplest feasible approach, the combination of the two previous limiting cases, where the outer free-draining shell of each blob describes the penetration of the flow. With the penetration depth d we have identified a new relevant parameter, which here is taken to be constant but which may also have to vary along the chain for a faithful quantitative description of real polymers. The velocity dependence of the overall polymer elongation $L(v)$ is modified by this generalization and simple power laws for $L(v)$, as predicted by approximations to former blob models, cannot be expected for polymers with a number of $N \sim 1500$ – 2000 Kuhn segments which are used in experiments. Only for much longer model chains there will be a small range of rather large flow velocities where a power law for $L(v)$ holds. However, in this regime the polymer is already quite elongated and effects of semiflexibility of real polymers become important [14].

Here, only stationary properties of polymers are analyzed. The consequences of the presented models for the dynamics of the polymers, such as the determination of the relaxation spectra and modes, are discussed elsewhere.

Stimulating discussions with S. CHU, T. DUKE, B. DÜNWEIG, E. FREY, H. MÜLLER-KRUMBHAAR and R. WINKLER are gratefully acknowledged.

REFERENCES

- [1] LUMLEY J. L., *Annu. Rev. Fluid Mech.*, **1** (1969) 367; VIRK P. S., *AIChE J.*, **21** (1975) 625; BERMAN N. S., *Annu. Rev. Fluid Mech.*, **10** (1978) 47; DEGENNES P.-G., *Physica A*, **140** (1986) 9.
- [2] BIRD R. B., ARMSTRONG R. C. and HASSAGER O., *Dynamics of Polymeric Liquids*, Vols. I, II, 2nd edition (John Wiley & Sons, New York), 1987.
- [3] DOI M. and EDWARDS S. F., *The Theory of Polymer Dynamics* (Clarendon Press, Oxford) 1986.
- [4] MÜLLER H. W. and ZIMMERMANN W., *Europhys. Lett.*, **45** (1999) 169.
- [5] PERKINS T. T., QUAKE S. R., SMITH D. E. and CHU S., *Science*, **264** (1994) 822; PERKINS T. T., SMITH D. E., LARSON R. G. and CHU S., *Science*, **268** (1995) 83; MANNEVILLE S. *et al.*, *Europhys. Lett.*, **36** (1996) 413; PERKINS T. T., SMITH D. E. and CHU S., *Science*, **276** (1997) 2016; QUAKE S. R., BABCOCK H. and CHU S., *Nature*, **388** (1997) 151.
- [6] ÖTTINGER H. C., *J. Chem. Phys.*, **86** (1987) 3731; *Rheol. Acta*, **35** (1996) 134. LARSON R. G., PERKINS T. T., SMITH D. E. and CHU S., *Phys. Rev. E*, **55** (1997) 1794.
- [7] BROCHARD-WYART F., *Europhys. Lett.*, **23** (1993) 105; **30** (1995) 387.
- [8] HENDRIKS J., KAWAKATSU T., KAWASAKI K. and ZIMMERMANN W., *On Semiflexible Polymers in an Anisotropic Medium: A Phenomenological Model*, unpublished, 1998.
- [9] RZEHAK R., KROMEN W., KAWAKATSU T. and ZIMMERMANN W., submitted to *Eur. Phys. J. B*.
- [10] WEEKS J. D., CHANDLER D. and ANDERSEN H. C., *J. Chem. Phys.*, **54** (1971) 5237.
- [11] GREST G. S. and KREMER K., *Phys. Rev. A*, **33** (1986) 3628; KREMER K. and GREST G. S., *J. Chem. Phys.*, **92** (1990) 5057; DÜNWEIG B. and KREMER K., *J. Chem. Phys.*, **99** (1993) 6983.
- [12] ZIMM B. H., *J. Chem. Phys.*, **24** (1956) 269.
- [13] PINCUS P., *Macromolecules*, **9** (1976) 386; **10** (1977) 210.
- [14] MARKO J. F. and SIGGIA E. D., *Macromolecules*, **28** (1995) 8759.